Magnetization reversal in nanoscale magnetic films with perpendicular anisotropy

Roger D. Kirby, J. X. Shen, R. J. Hardy, and D. J. Sellmyer

Behlen Laboratory of Physics and Center for Materials Research and Analysis, University of Nebraska, Lincoln, Nebraska 68588-0111

We present experimental results on magnetization reversal for a class of nanoscale magnetic films with perpendicular magnetic anisotropy and develop a model that describes a variety of related experiments. In this model the sample is divided into identical single domain cells that interact through dipolar fields and a nearest-neighbor domain-wall interaction. Monte Carlo simulations give insights into the relationship between the macroscopic magnetic parameters and the reversal behavior and demonstrate the important role that thermal activation plays in the reversal process.

Among the most exciting advances in modern condensed-matter and materials physics is the incipient development of an ability to understand and design structures with nanometer-length scales.[1-3] These structures and the technologies based on them will be important in areas such as information storage,[4] electronic devices,[5] and biotechnology.[6] As the dimensions of the fundamental building blocks or cells of magnetization, polarization, etc., become smaller and smaller, the temporal stability of an ordered phase within the cell becomes of crucial importance. This problem is also intimately connected to the mechanism by which a reversal or switch of the order parameter in the cell occurs as the result of an applied stimulus.

This paper is concerned with time decay and reversal phenomena in an important class of nanostructured thin films, amorphous magnetic multilayers with characteristic layer thicknesses of a few atomic diameters. Such films have considerable potential in future ultra-high-density magneto-optic data storage systems.

Magnetization reversal has been studied in a number of nanostructured thin-film and amorphous rare-earth–transition-metal systems.[7-12] These earlier measurements explicitly show that the reversal behavior in these systems tends to fall between one of two limiting categories: (a) continuous nucleation with the magnetization varying approximately as $\ln(t)$ for a significant period of time, and (b) slow nucleation followed by rapid domain growth.

These two limiting behaviors are illustrated in Fig. 1 for Dy/Fe compositionally modulated multilayer samples, where the polar Kerr angle θ_K, which is proportional to the magnetization M, is plotted as a function of time.[11] These measurements were carried out by first saturating the sample with a large magnetic field perpendicular to the film and then reversing the field to a value near the coercive field H_c (the applied field for which $M=0$) and holding it constant while the Kerr rotation was monitored. The dashed line shows the time dependence of the polar Kerr rotation of a Dy(5 Å)/Fe(8.1 Å) sample, which illustrates type-(a) behavior. The Kerr rotation completely reverses only for applied fields greater than the saturation field (the applied field for which θ_K first reaches its maximum value), and at longer times the

magnetization varies approximately as $\ln(t)$. In contrast, the solid line shows the time dependence of the polar Kerr rotation of a Dy(5 Å)/Fe(5.6 Å) sample, which completely reverses even for applied field well below the coercive field. The shape of the reversal curve suggests type-(b) behavior. The inset in Fig. 1 shows part of hysteresis loops observed by Kerr rotation for the two samples. The Dy(5 Å)/Fe(5.6 Å) sample shows a much more rapid switching transition.

This paper develops a simple uniaxial anisotropy model that can describe the observed reversal behaviors in Dy/Fe and similar systems. The model can be used to calculate hysteresis loops and time and magnetization reversal curves, and it leads to insights into the magnetic behaviors of such thin films.

Consider an amorphous thin-film ferromagnet with perpendicular magnetic anisotropy. Both experimentally and theoretically, we consider only external magnetic fields **H** that are perpendicular to the plane of the film and thus parallel to the easy axis. The total energy of a uniformly magnetized film is[3,13]

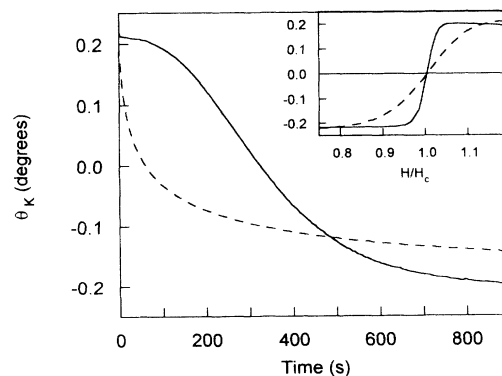$$E = K_u V \sin^2\theta - M_s V(H - NM_z)\cos\theta , \qquad (1)$$

FIG. 1. Measured Kerr rotation angle as a function of time after field reversal for Dy(5 Å)/Fe(5.6 Å) (solid line) and Dy(5 Å)/Fe(8.1 Å) (dashed line) multilayers at room temperature. The inset shows the Kerr rotation switching transitions for the same two samples at a field sweep rate of 140 Oe/s.

<u>49</u>   10 810

MAGNETIZATION REVERSAL IN NANOSCALE MAGNETIC . . .

where θ is the angle between the magnetization **M** and the field **H**. The z component of **M** is M_z, where the z axis is perpendicular to the plane of the film. The magnitude of the magnetization is assumed to have a constant value of M_s, the saturation magnetization. N is the demagnetizing factor, V is the total film volume, and K_u is the perpendicular anisotropy constant. Equation (1) has minima at $\theta=0$ and π for positive K_u, provided that $2K_u > M_s|H-NM_z|$. Lottis, White, and Dahlberg[3] and Lyberatos, Chantrell, and Hoare[14] used Eq. (1) to study a thin film containing aligned and highly anisotropic single domain particles with reversal occurring by thermal activation of the particulate moments over an anisotropy barrier. The only particle-particle interactions included in their calculations were the dipolar interactions.

We assume that Eq. (1) describes the energy of a uniform thin magnetic film on a *mesoscopic* scale, specifically, that it applies to small volumes that extend through the thickness of the film. These volumes will be referred to as "cells." The individual atomic moments within a cell are strongly coupled by exchange, so they tend to rotate coherently during a thermal fluctuation. The volumes of the cells are assumed to be sufficiently large that there is considerable averaging of their spatially varying composition and anisotropy, so that similarly sized cells can be treated in the same way. Because of thermal fluctuations, the magnetization of the film will reverse locally by thermal activation. In the process domain walls will form around the cells at the expense of both exchange and anisotropy energy. A term is needed to account for the energy involved in the formation of these walls.

We first divide the sample into N identical single domain cells of volume V_c on a hexagonal lattice, so that each cell interfaces with six other cells. The magnitude of the magnetic moment of each cell is M_sV_c. Except during the reversal process, the moment of each cell will be aligned along the $+z$ or $-z$ directions. For cell j these two possibilities will be specified by $m_j=+1$ or -1, respectively. For simplicity we assume that the individual atomic moments within a cell rotate coherently while the orientations of the moments in the other cells remain fixed along the $\pm z$ directions. We propose that the energy of cell j during the reversal process be taken to be

$$E_j = K_u V_c \sin^2\theta_j - M_s V_c (H_z + \hat{H}_j)\cos\theta_j$$
$$+ \tfrac{1}{6}(3 - \tfrac{1}{2}S_j\cos\theta_j)E_w , \qquad (2)$$

where θ_j is measured from the $+z$ axis. When initially $m_j=+1$, reversing changes θ_j from 0 to π and changes $\cos\theta_j$ from $+1$ to -1, and when initially $m_j=-1$, reversing changes $\cos\theta_j$ from -1 to $+1$. Thus, the initial value of $\cos\theta_j$ equals the initial value of m_j. E_w is the energy needed to form a domain wall on all six edges of a cell. $S_j=\sum_k m_k$ is a sum over the six nearest neighbors of cell j and ranges in value from -6 to $+6$. Note that $(3-\tfrac{1}{2}S_j m_j)$ is the initial number of faces on cell j that possess domain walls. $H_z=\pm|\mathbf{H}|$ is the z component of the external field, and $\hat{H}_j$ is the demagnetizing field at the

center of cell j caused by all other cells in the sample. In the simulations described below, $\hat{H}_j$ is calculated in the point dipole approximation. More complicated expressions for the wall energy could be considered, but the above simple form produces domain growth similar to that observed experimentally. Energy terms similar to ours have been considered earlier in equilibrium calculations of thermomagnetic reversal in rare-earth–transition-metal films.[15]

Equation (2) has minima at $\theta_j=0$ and π with a maximum in between. The energy barrier to reversal is the difference in energy between the initial minimum and the maximum. It is given by

$$E_j^B = K_u V_c \left[1 + m_j \left(\frac{M_s V_c (H_z + \hat{H}_j) + \tfrac{1}{12}S_j E_w}{2K_u V_c} \right) \right]^2 , \qquad (3)$$

where m_j gives the initial direction of the magnetization of the cell. For an isolated cell to reverse, walls must be formed on all six of its faces, which requires considerable energy. If a cell reverses adjacent to already reversed cells, fewer new walls are needed and the energy barrier is reduced.

To calculate the time dependence of the reversal process, we assume that thermal fluctuations cause the cells to reverse their magnetization by "jumping" over the energy barriers. The probability that cell j reverses its magnetization in time Δt is

$$P_j = R \exp(-E_j^B/k_B T)\Delta t , \qquad (4)$$

where R is an attempt frequency, which is assumed to be the same for reversing in either direction and is chosen to be 2×10^9 s^{-1}, which is a typical value. T is temperature and k_B is Boltzmann's constant. In the simulations the time interval Δt in Eq. (4) is determined by first calculating the transition rate $P_j/\Delta t$ for all cells, and then choosing Δt to make P_j equal to $1/N$ for the cell with the maximum transition rate. A cell is then chosen at random, so that each cell is chosen with probability $1/N$. The value of NP_j for the chosen cell is compared with a random number distributed uniformly between 0 and 1. When NP_j is greater than or equal to the random number, the chosen cell is reversed, otherwise it is not. Time t is then advanced by Δt and the calculation is repeated. The transition rates only require recalculating when a cell has been reversed, or if the external field is being continuously changed.

The time dependence of magnetization reversal is calculated by first saturating the sample, so that $m_j=+1$ for all cells. The external field is then switched to the $-z$ direction and the reversals of the cells are observed. Hysteresis loops are calculated by changing the external field linearly with time throughout the simulation. A rate of 200 Oe/s was used, which is a typical experimental value. It should be emphasized that in these simulations the rate of approach to thermodynamic equilibrium is limited by thermal activation, so that the decay phenomena occurs on the experimentally observed time scale of $\sim 10^3$ s. This time scale is very different from the time scale of $\sim 10^{-9}$ s typical of solutions of the Landau-Lifshitz-Gilbert equation for a collection of interacting magnetic

moments.[16]

The dipole-dipole interaction between cells is calculated directly for cells out to third neighbors, with the contribution of the remainder being calculated in the mean-field approximation. However, we found that calculating all interactions in the mean-field approximation did not qualitatively affect the results obtained.

Figure 2 shows calculated reversal curves for two different values of E_w, assuming typical values[17] for K_u and M_s, namely, $K_u = 1.0 \times 10^6$ erg/cm^3 and $M_s = 90$ emu/cm^3. In each case, the volume V_c was adjusted to give a room-temperature coercivity close to 7 kOe, which is similar to the measured coercivities of the samples in Fig. 1. The magnetization reversal curve for $E_w = 2 \times 10^{-13}$ erg (dashed line) is similar to the type-(a) reversal curve for Dy(5 Å)/Fe(8.1 Å) in Fig. 1. The calculated magnetization varies approximately as $\ln(t)$ from 280 to 2800 s. This quasilogarithmic behavior arises because the demagnetizing field changes as the reversal proceeds. As was shown earlier by Lottis, White, and Dahlberg,[3] a distribution of relaxation times is not necessary for this type of time dependence. The reversal curve for the larger wall energy of $E_w = 8 \times 10^{-13}$ erg (solid line) has a significantly different character and is qualitatively similar to the type-(b) experimental curve for Dy(5 Å)/Fe(5.6 Å). It has an initial slow reversal rate followed by a rapid reversal rate. (In this simulation the anisotropy field $2K_u/M_s$ is 22.2 kOe; the reduction of H_c from this value is caused by thermal activation.) The inset in Fig. 2 shows the simulated $-M_s$ to $+M_s$ switching transitions. The $E_w = 2 \times 10^{-13}$ erg curve (dashed line) shows a slow switching transition from the $-M_s$ state to the $+M_s$ state, while the $E_w = 8 \times 10^{-13}$ erg curve (solid line) shows a much more rapid transition.

The domain patterns obtained in the simulations justify the characterization of the experimental behavior shown in Fig. 1 as either reversal by continuous nucleation or reversal by slow nucleation followed by rapid domain growth. The black regions in Fig. 3 indicate cells that have reversed. Figure 3(a) shows the domain pattern for

E$_W$=2x10^{-13} erg   E$_W$=8x10^{-13} erg

FIG. 3. Simulated reversed domain patterns at 30% reversal for the same two sets of parameters used to obtain Fig. 2.

$E_w = 2 \times 10^{-13}$ erg at 30% reversal. Since there is only a small preference for cells to reverse near already reversed cells, the process is dominated by the continuous reversal of isolated cells (or nuclei). Figure 3(b) shows the domain pattern for $E_w = 8 \times 10^{-13}$ erg at 30% reversal. Only a few large domains have formed. Since the probability of a cell reversing is much greater for cells adjacent to already reversed cells, domains grow rapidly around any cell that by chance has been reversed. These simulated domain patterns strongly resemble experimental domain patterns observed by Labrune, Andrieu, and Bernstein.[9]

Figure 4(a) shows the room-temperature experimental results for the dependence of the coercive field H_c on the logarithm of the magnetic-field sweep rate during the hysteresis loop measurement for a Dy(5 Å)/Fe(5 Å) sample, which is similar to the type-(b) sample discussed above. Note that the measured H_c increases by nearly 20% as the sweep rate is changed over the range obtainable with our apparatus. Figure 4(b) shows a similar dependence obtained in a simulation. The significant dependence of the coercivity on the sweep rate is strong evidence that the reversal process is not an equilibrium process, and the similarity of the experimental and simu-
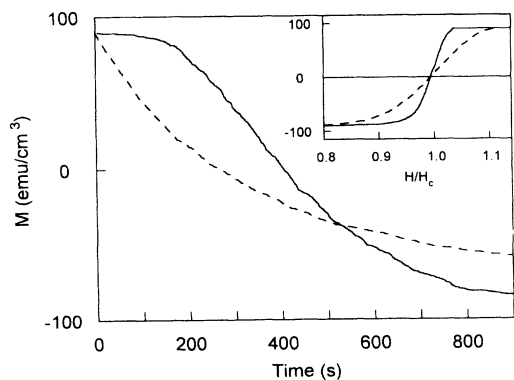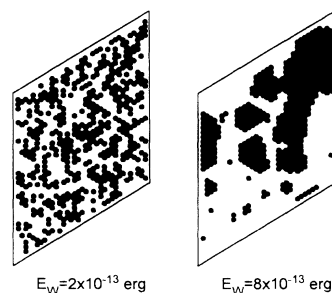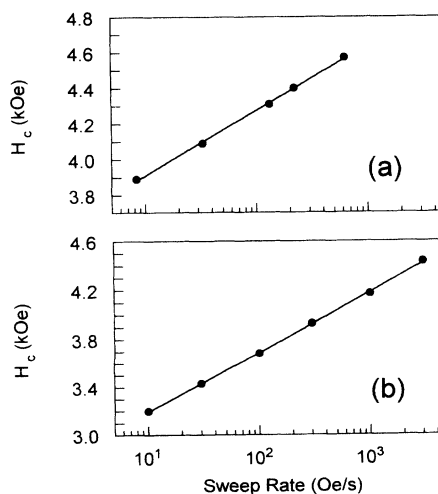

FIG. 2. Simulated magnetization reversal curves for $E_w = 2 \times 10^{-13}$ erg (dashed line) and $E_w = 8 \times 10^{-13}$ erg (solid line) at room temperature. $V_c = 1.96 \times 10^{-18}$ and 1.70×10^{-18} cm^3, respectively. $M_s = 90$ emu/cm^3 and $K_u = 1 \times 10^6$ erg/cm^3 for both curves. The inset shows the corresponding switching transitions at a field sweep rate of 200 Oe/s.

FIG. 4. Coercive field vs field sweep rate. (a) Experimental results for Dy(5 Å)/Fe(5 Å). (b) Simulation results for $M_s = 90$ emu/cm^3, $K_u = 0.6 \times 10^6$ erg/cm^3, $E_w = 2 \times 10^{-13}$ erg, and $V_c = 3 \times 10^{-18}$ cm^3. (V_c was chosen to give a coercivity close to the experimental value.) The lines between points are guides to the eye.

lational results is evidence that thermal activation is the principal nonequilibrium process involved. Further work on quantitative fits to the experimental data, including the temperature dependence of the coercivity, will be reported elsewhere.[18]

There are some other important aspects of this investigation which should be mentioned. (1) It is somewhat surprising that such a simple model of magnetization reversal is capable of describing these complex magnetic systems for which random variations in the local magnetic properties such as anisotropy and exchange interactions are known to be important. The likely reason for the model working so well is that the individual cells do in fact experience a range of activation energies. These arise from the changing demagnetizing field and from the different numbers of reversed nearest neighbors. When the range of activation energies caused by these effects is large compared to the variations caused by the randomness in the anisotropy and exchange interactions, one expects that the latter effects will be of secondary importance. (2) A general observation is that the shapes and decay rates of the simulated constant-field magnetization vs time curves are much more sensitive to the model parameters than are the shapes of the hysteresis loops. This result will likely be true for any theory of magnetization reversal, and it suggests that magnetization vs time measurements will provide the more useful test of any theory. (3) Relaxation in magnetic and glassy systems has also been treated through scaling models of reversal[19] and in models involving hierarchically constrained dynamics.[20] Such approaches usually lead to power-law or stretched exponential relaxation. Many of our simulation and experimental results can be described by such approaches, and it would be of interest to investigate the connection between the model presented here and these earlier approaches.

In summary, we have presented experimental results and a uniaxial anisotropy model for describing magnetization reversal in nanostructured magnetic films. The goal of the simulations to date has been to use the simplest possible model to provide a semiquantitative picture of the magnetization reversal process in amorphous thin-film magnetic systems. To our knowledge, this is the first investigation where the details of hysteresis loop measurements and constant-field magnetization vs time measurements have been simultaneously and reasonably successfully described in real magnetic systems. Moreover, the simulations explicitly demonstrate the importance of thermal activation in the reversal process. The model developed here, with suitable modifications, may also be relevant to such systems as Co/Pt multilayers,[12] Au/Co/Au trilayers,[2] and particulate materials like Co/Cr where interparticle exchange interactions may be important, as well as other nanostructured systems currently being considered as high-density magneto-optic storage media.

[1]For review, see the articles in Phys. Today 45 (10) (1992).

[2]J. Pommier, P. Meyer, G. Pénissard, J. Ferré, P. Bruno, and D. Renard, Phys. Rev. Lett. 65, 2054 (1990).

[3]D. K. Lottis, R. White, and E. D. Dahlberg, Phys. Rev. Lett. 67, 362 (1991).

[4]L. M. Falicov et al., J. Mat. Res. 5, 1299 (1990).

[5]M. A. Reed, Sci. Am. xx, 118 (1993).

[6]H. Hollis Wickman, APS News 2, 22 (1993), and references therein.

[7]K. Ohashi, H. Tsuji, S. Tsunashima, and S. Uchiyama, Jpn. J. Appl. Phys. 19, 1333 (1980).

[8]G. A. N. Connell and R. Allen, in Proceedings of the 4th International Conference on Rapidly Quenched Metals, Sendai, 1981, edited by editors (publisher, city, 19xx), p. 981.

[9]M. Labrune, S. Andrieu, and P. Bernstein, J. Magn. Magn. Mater. 80, 211 (1989).

[10]T. Thomson, K. O'Grady, S. Brown, P. W. Haycock, and E. W. Williams, IEEE Trans. Magn. 28, 2515 (1992).

[11]R. D. Kirby, J. Shen, Z. Shan, and D. J. Sellmyer, J. Appl. Phys. 70, 6200 (1991).

[12]J. X. Shen, R. D. Kirby, K. Wierman, Z. S. Shan, D. J. Sellmyer, and T. Suzuki, J. Appl. Phys. 73, 6418 (1993).

[13]F. C. Stoner and E. P. Wohlfarth, Philos. Trans. A 240, 599 (1948).

[14]A. Lyberatos, R. W. Chantrell, and A. Hoare, IEEE Trans. Magn. 26, 222 (1990).

[15]M. Mansuripur, J. Appl. Phys. 61, 1580 (1987).

[16]M. Mansuripur, R. C. Giles, and G. Patterson, J. Magn. Soc. Jpn. 15, 17 (1991).

[17]Z. S. Shan and D. J. Sellmyer, Phys. Rev. B 42, 10 433 (1990).

[18]R. D. Kirby, J. X. Shen, R. J. Hardy, and D. J. Sellmyer (unpublished).

[19]R. V. Chamberlin and R. Holtzberg, Phys. Rev. Lett. 67, 1606 (1991).

[20]R. G. Palmer, D. L. Stein, E. Abrahams, and P. W. Anderson, Phys. Rev. Lett. 53, 958 (1984).